J Incl Phenom Macrocycl Chem (2010) 67:133–140
DOI 10.1007/s10847-009-9688-5

ORIGINAL ARTICLE

Complexation of metal ions with the novel diazadithia crown ether carrying two anthryl pendants in acetonitrile–tetrahydrofuran

Semanur Parlayan · Aysel Başoğlu · Miraç Ocak · Hakan Alp · Halit Kantekin · Ümmühan Ocak

Received: 6 August 2009 / Accepted: 4 October 2009 / Published online: 15 October 2009

Abstract A new crown ether carrying two anthryl groups with nitrogen–sulfur donor atom was designed and synthesized by the reaction of the corresponding macrocyclic compound and 9-chloromethyl anthracene. The influence of metal cations such as Al^{3+}, Zn^{2+}, Fe^{2+}, Fe^{3+}, Co^{2+}, Ni^{2+}, Mn^{2+}, Cu^{2+}, Cd^{2+}, Hg^{2+} and Pb^{2+} on the spectroscopic properties of the ligand was investigated in acetonitrile–tetrahydofuran solution (1/1) by means of absorption and emission spectrometry. Absorption spectra show isosbestic points in the spectrophotometric titration of Fe^{2+}, Fe^{3+}, Al^{3+}, Cu^{2+} and Hg^{2+}. The results of spectrophotometric titration experiments disclosed the complexation stoichiometry and complex stability constant of the novel ligand with Fe^{2+}, Fe^{3+}, Al^{3+}, $Cu^{2+}$and Hg^{2+}cations. The presence of excess amounts of Al^{3+}, Zn^{2+}, Fe^{2+}, Fe^{3+}, Co^{2+}, Ni^{2+}, Mn^{2+}, Cu^{2+}, Cd^{2+}, Hg^{2+} and Pb^{2+} cations caused an enhancement of anthryl fluorescence. The ligand showed good sensitivity for Zn^{2+} with respect to other metal cations with linear range and detection limit of 1.4×10^{-7} to 4.1×10^{-6} M and 1.0×10^{-8} M respectively.

Keywords Crown ether · 9-chloromethyl anthracene · Fluorescence spectroscopy · Stability constant · Metal cation

S. Parlayan · M. Ocak · H. Kantekin · Ü. Ocak (✉)
Department of Chemistry, Faculty of Arts and Sciences, Karadeniz Technical University, 61080 Trabzon, Turkey
e-mail: ummuhanocak@yahoo.com

A. Başoğlu
Bayburt University, Vocational School, Bayburt, Turkey

H. Alp
Karadeniz Technical University, Maçka Vocational School, Maçka, Trabzon, Turkey

Introduction

Most transition metal cations are known to be hazardous pollutants with toxic effects for the living organisms in environmental systems [1–5]. The toxicity of mercury is well-known for many years. Mercury and its compounds have been used in industrial applications. Chronic exposure to inorganic mercury salt causes serious problems on both the physiological and the neurological systems of the human body [6]. Iron between other transition metals is a moderately toxic element. However, toxic doses of iron and its compounds can lead to serious health problems [6]. Aluminum is potentially neurotoxic [7–9]. On the other hand, zinc plays an important role in neurobiology [10]. Zinc is associated with the developing brain and central nervous system [11]. Therefore, zinc is the most important element among the trace elements in human nutrition. It is vital for the immune system, the expression of genes and the transfer of nervous signals [12]. Zinc is used often in industry because of its chemically active nature. The widespread use of zinc has led to increased monitoring of zinc levels in the environmental systems. The determination of traces of zinc is important in quality control for the chemical and metallurgical industries. Therefore, new methods and reagents for selective determination of hazardous metal cations in the environment have appeared to have great scientific aims. There are several methods that can determine zinc at trace levels in a variety of samples. Flame atomic absorption spectrometry, spectrofluorimetry, adsorptive stripping voltametry, have been used for the determination of zinc [13–15]. The high selectivity and sensitivity of spectrofluorometric methods make them very appealing for the detection and quantification of heavy metals [16–18].

Fluorescent chemosensors for cations usually consist of an ionophore and a fluorophore part. The ionophore part is able to recognize a target cation selectively and the fluorophore part is able to convert the recognition of cation into optical signals. This conversion can be explained by several types of photophysical mechanisms such as photo-induced electron transfer (PET), photo-induced charge transfer (PCT) and excimer formation [19].

Crown ether compound are well-known as selective macrocyclic ligands for cation recognition [20–24]. Selectivity depends on some factors such as cation-cavity match, donor atom types in crown cavity and cation properties. Classical crown ether ligands, which have oxygen donor atoms, show selective complexation with alkali and alkaline earth metal cations. However, crown ethers having sulfur and nitrogen donor atoms are able to undergo complexation with soft metal cations.

Anthracene and its derivatives have been used as fluorophore groups in the design of fluorescent cation chemosensors [25–28]. These groups have shown very interesting photo-physical properties [29, 30]. In the present study we report the preparation of a novel crown ether ligand having two anthryl side arms with nitrogen–sulfur mixed donor, **(3)**, and present the complexation properties of the ligand with a series of metal cations. The complex stability constants and complex compositions of metal cations with the ligand were determined by using spectrophotometric titrations in acetonitrile–tetrahydrofuran solution (1/1). We propose the new ligand for the determination of zinc.

Experimental

Chemicals

Acetonitrile and tetrahydrofuran from Merck (spectrometric grade) were the solvents for absorption and fluorescence measurements. All metal perchlorates purchased from Acros were of the highest quality available and vacuum dried over blue silicagel before use. 9-chloromethyl anthracene was purchased from Aldrich.

Apparatus

^{1}H NMR spectra were recorded on a Varian 200 A spectrometer, using $CDCl_3$ with TMS as the internal reference. IR spectra were recorded on a Perkin-Elmer 1600 FTlR spectrophotometer using KBr pellets. Elemental analysis was performed on Costech 4010 CHNS instrument. The absorption spectra of the solutions were recorded using a Unicam UV2 model spectrophotometer. A Photon Technologies International Quanta Master Spectrofluorimeter (model QM-4/2006) was used for all fluorescence measurements.

Measurements

Absorption spectra of the ligand **(3)** with a concentration of 2.58×10^{-5} M in acetonitrile–tetrahydrofuran solution (1/1) containing 10 molar equivalents of appropriate metal perchlorate salt were measured using 1-cm absorption cell. Fluorescence spectra of the ligand solutions of 1.93×10^{-6} M were measured in 1-cm quartz cell. Excitation wavelength was 368 nm for **(3)**. Fluorescence emission spectra were recorded in the range 380–500 nm with slit width 1.0 nm.

The stoichiometry of the complexes was determined by using the molar-ratio method. The stability constants were calculated according to the procedure described in literature [31].

Synthesis

Synthesis of the ligand (3)

Compound **(1)** [32] (0.50 g, 1.39 mmol) was dissolved in dry tetrahydrofuran (15 mL) and purged under nitrogen atmosphere in a Schlenk system connected to a vacuum line. A solution of 9-chloromethyl anthracene **(2)** (0.71 g, 3.13 mmol) in dry tetrahydrofuran (15 mL) was added dropwise to this solution for 30 min. at 40 °C. Triethylamine (0.85 g, 8.41 mmol) was added to the mixture. The reaction mixture was refluxed and stirred at reflux temperature for 47 h, and monitored by TLC [silica gel, dichloromethane:ethyl alcohol (17:1)]. At the end of this period, the reaction mixture was filtered. The filtrate was concentrated on an evaporator to 10 mL and the solid formed was filtered off, washed with cold diethyl ether, then dried in vacuo. The pale yellow solid product (yield 98.8%) was obtained by recrystallization from benzene, mp 210–212 °C. Anal. Calc.for $C_{50}H_{46}N_2S_2$: C, 81.30; H, 6.23; N, 3.79; S, 8.67%. Found: C, 81.35; H, 6.27; N, 3.95; S, 8.42%. IR (KBr disk, cm^{-1}): 3056–3029 (Ar–H), 2942–2813 (C–H), ^{1}H-NMR ($CDCl_3$) : (δ) 7.00–7.36 (m, 8H, macrocyclic Ar–H), 7.36–8.39(m, 18H, anthracene Ar–H) 4.51 (s, 4H, anthracene–CH_2), 3.76 (s, 4H, benzene–CH_2), 2.58–2.68 (m, 8H, N–CH_2 and S–CH_2), 1.87 (m, 4H, C–CH_2–C).

Results and discussion

Characterization of the ligand (3)

The synthetic pathway to the new ligand **(3)** is summarized in Scheme 1. Compound **(1)** was prepared according to the literature [32].

Compound **(3)** was synthesized by the reaction of the compound **(1)** with 9-chloromethyl anthracene **(2)** in dry THF. The absence of the secondary amine band belonging to starting material **(1)** in the IR spectra of the crown ether **(3)** with anthryl side arms has supported the structure. In the ^{1}H-NMR spectrum of **(3)**, the singlets (4H each) belong to methylene protons of anthryl groups and benzylic methylene protons are observed at $\delta = 4.52$ ppm and $\delta = 3.76$ ppm, respectively. The multiplet (8H) between $\delta = 2.58$ ppm and $\delta = 2.68$ ppm belongs to N–CH_2 and S–CH_2 protons. The multiplet (4H) at $\delta = 1.87$ ppm belongs to C–CH_2–C protons. Elemental analysis results confirm the proposed structure.

Absorption spectra

The absorption spectra of the ligand **(3)** in acetonitrile–THF (1/1) display the strong π–π^* absorption bands at 330–400 nm characteristic of the pendant anthracenyl groups [33]. As seen from Fig. 1, the ligand **(3)** possesses four absorption bands at 334, 350, 368 and 388 nm. Molar absorption coefficients are, 5.4×10^3, 9.9×10^3, 1.6×10^4 and 1.5×10^4 cm^{-1} M^{-1} in these wavelengths, respectively.

The presence of 10 equivalents of Cd^{2+}, Co^{2+}, Ni^{2+}, Mn^{2+}, Zn^{2+} and Pb^{2+}cations produces modest changes in the absorption of the ligand (Fig. 2). These metal cations caused a decrease of absorption at 350, 368 and 388 nm. The effects of Cu^{2+}, Hg^{2+}, Al^{3+}, Fe^{2+} and Fe^{3+} ions on the absorption spectra of the ligand are pronounced. As seen from Fig. 2, the interaction of Fe^{3+} and Fe^{2+} with the ligand is nearly similar. These cations markedly decreased absorptions at 368 and 388 nm. However, an increase of absorption at 350 was observed for Fe^{3+} and Fe^{2+}. The effect of Cu^{2+}, Hg^{2+} and Al^{3+} is similar. These cations caused a pronounced decrease of absorption for all the absorption maxima. On the other hand, there was a little

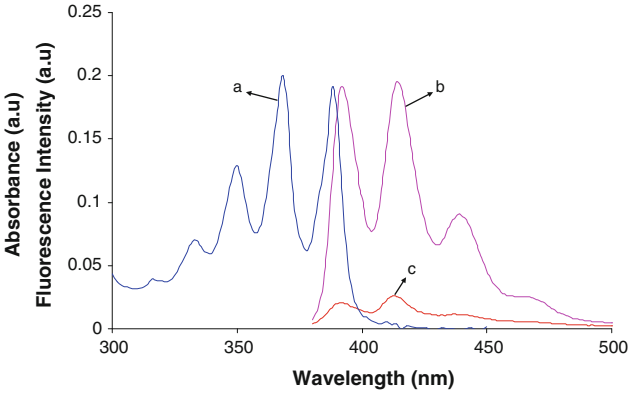

Fig. 1 UV absorption (a) and emission spectra (c) of the ligand **(3)** in acetonitrile–tetrahydrofuran solution (1/1). Ligand concentrations were 2.58×10^{-5} M and 1.93×10^{-6} M for absorption and emission spectra, respectively. Excitation wavelength is 368 nm. b shows fluorescence spectra of a solution of 1.93×10^{-6} M of 9-chloromethyl anthracene in acetonitrile–tetrahydrofuran (1/1)

blue shift for the 388 nm absorption band for Cu^{2+}, Hg^{2+}, Al^{3+}, Fe^{2+} and Fe^{3+} ions. Similar effect was also observed for the 350 nm absorption band in case of Cu^{2+} and Hg^{2+}. It is interesting that Cu^{2+}, Hg^{2+}, Al^{3+}, Fe^{2+} and Fe^{3+} ions caused a new broad absorption band at 394 nm. These results show that Cu^{2+}, Hg^{2+}, Al^{3+}, Fe^{2+} and Fe^{3+} interact with anthracene groups of the ligand **(3)**.

Spectrophotometric titrations

We found a regular change in the absorption spectra of the ligand **(3)** with increasing concentrations of Fe^{2+}, Fe^{3+}, Al^{3+}, Cu^{2+} and Hg^{2+}. It is interesting that the effect of excess amounts of these cations on the absorption spectra of the ligand **(3)** is similar. As seen from Fig. 2, the mentioned cations cause a collapse at the 368 and 388 nm absorption bands. We could not found a regular change in the absorption spectra of the ligand **(3)** with increasing

Scheme 1 Synthetic pathway to the new crown ether ligand **(3)** used in this study

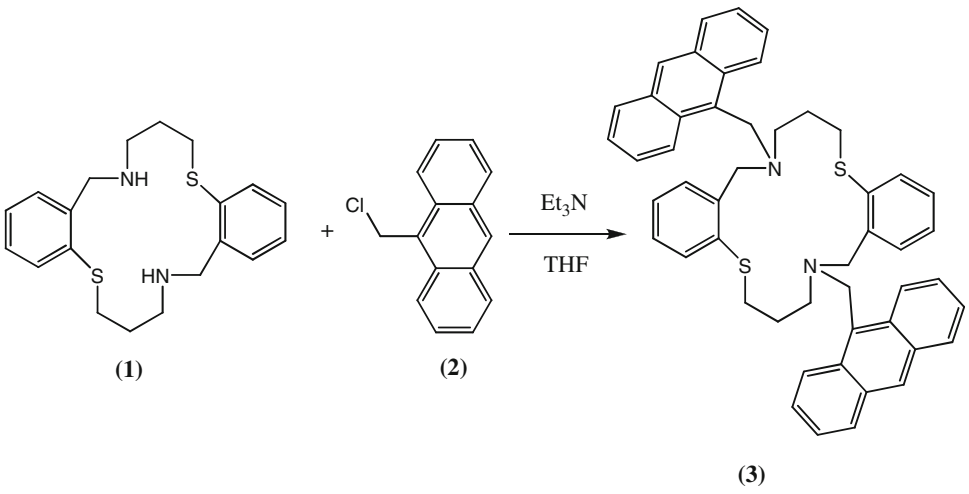

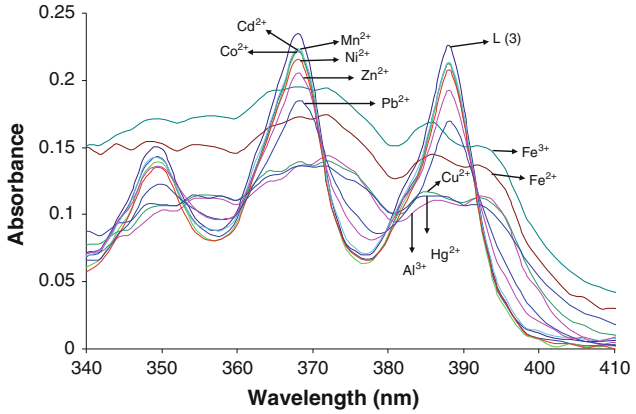

Fig. 2 The effect of metal cations on the absorption spectra of **(3)** in acetonitrile–tetrahydrofuran solution (1/1). Ligand concentration:2.58 × 10^{-5} M. Metal perchlorate concentrations:2.58 × 10^{-4} M

concentrations of Zn^{2+}, Ni^{2+}, Mn^{2+}, Co^{2+}, Cd^{2+} and Pb^{2+} cations. It is interesting that the effect of excess amounts of these cations on the absorption spectra of the ligand **(3)** is also similar. As seen from Fig. 2, the presence of 10 equivalents of these cations produces modest decreases in the absorption of 350, 368 and 388 nm.

The change in the absorption spectra of the ligand **(3)** with increasing concentrations of Hg^{2+} is shown in Fig. 3. There were five isosbestic points at 354, 362, 372, 382 and 392 nm. This result indicates that there were five equilibriums during the complexation. The isosbestic point at 392 nm is well-pronounced. Other isosbestic points were not clear when it was observed in detail. This seems to be due to the presence of small amounts of free ligand. The presence of many isosbestic points may result from different complex compositions. The decrease of absorbance at 368 nm provided the determination of the complex composition of the Hg^{2+}-ligand **(3)**. As seen from Fig. 3 (inset above), the inflection point was 2.0 ([M]/[L]). It can thus be concluded that ligand **(3)** formed a stable 2:1 (M:L) complex with Hg^{2+}. In order to determine the complex stability constant, the ratio of $A_o/(A_o - A)$ was plotted versus $[M]^{-1}$, as in Fig. 3 (inset below), which gave a good straight line. A_o and A are the absorbance of the free ligand and the absorbance of the solution involving Hg^{2+} cation, respectively. The stability constant was calculated from the ratio intercept/slope [31]. The value of log K was 4.48 for Hg^{2+}-complex.

Figure 4 shows the change in the absorption spectra of the ligand **(3)** with increasing concentrations of Fe^{2+}. The changes in the absorption spectra were a little different from that in the case of Hg^{2+} ion. There were two isosbestic points at 372 and 392 nm. This result indicates that there were only two equilibriums during the complexation with Fe^{2+}. These equilibriums may belong to two different complexes. Figure 4 (left inset) shows the molar ratio plot for Fe^{2+}. The inflection point was 2.0 ([M]/[L]). Therefore, we disclosed formation of a stable 2:1 (M:L) complex with Fe^{2+} from the absorbance changes at 368 nm. Figure 3 (inset right) shows the plot for calculation of the stability constant of this complex. The value of log K was 4.45 for the Fe^{2+}-complex.

The change in the absorption spectra of the ligand **(3)** with increasing concentrations of Fe^{3+} is shown in Fig. 5. The changes in the absorption spectra were similar to that in the case of Fe^{2+} ion. There were two isosbestic points at 372 and 392 nm indicating the presence of two equilibriums in solution. As seen from inset in left (break point is 2.0) the complex composition was 2:1 (M:L) for Fe^{3+}. The value of log K was 4.49 in case of Fe^{3+}-complex.

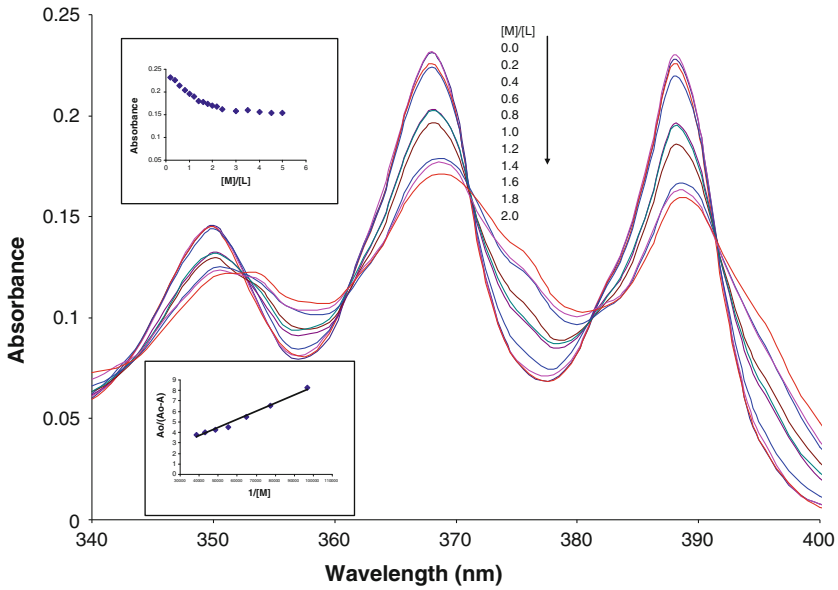

Fig. 3 Relationship of the absorbance of the ligand **(3)** with the concentration of Hg^{2+}. The spectral changes during the addition of 0–2 equivalents of $Hg(ClO_4)_2$. Ligand concentration: 2.58 × 10^{-5} M. *Insets*: Measurements were carried out at 368 nm

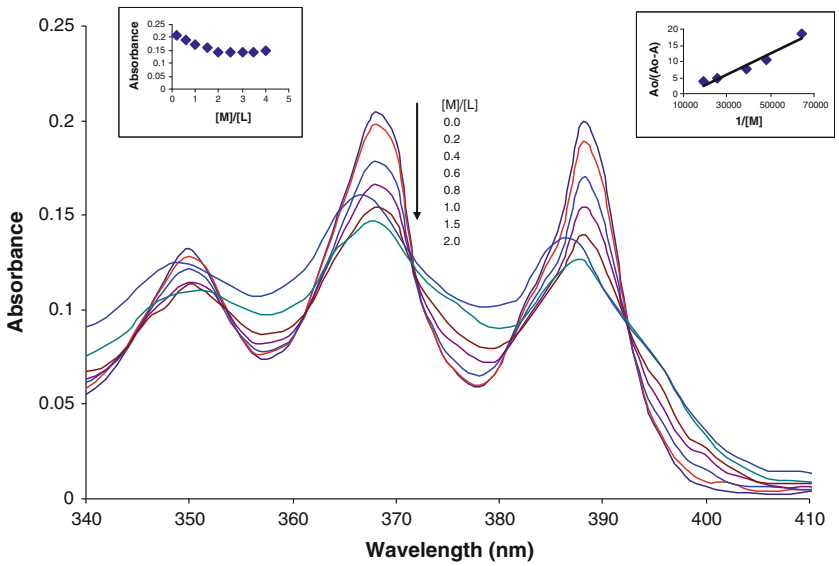

Fig. 4 Relationship of the absorbance of the ligand **(3)** with the concentration of Fe^{2+}. The spectral changes during the addition of 0–2 equivalents of $Fe(ClO_4)_2$. Ligand concentration: 2.58×10^{-5} M. *Insets*: Measurements were carried out at 368 nm

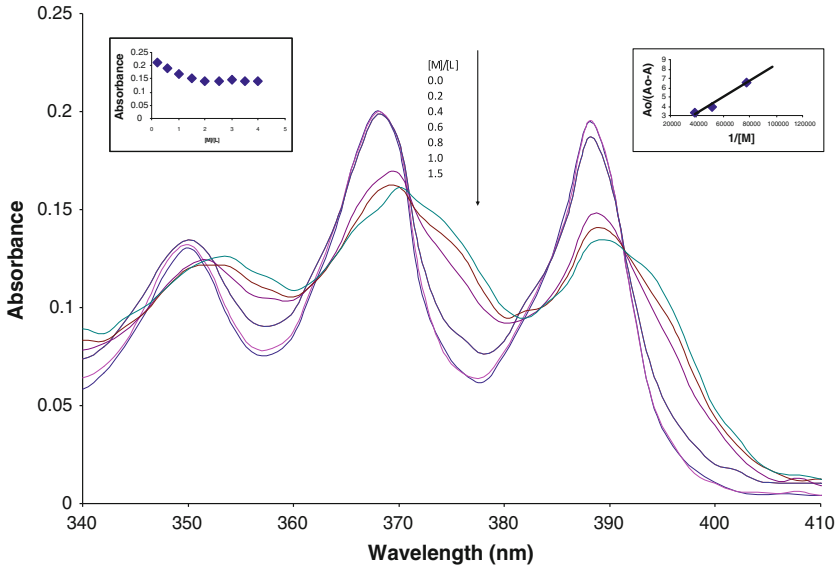

Fig. 5 Relationship of the absorbance of the ligand **(3)** with the concentration of Fe^{3+}. The spectral changes during the addition of 0–1.5 equivalents of $Fe(ClO_4)_3$. Ligand concentration: 2.58×10^{-5} M. *Insets*: Measurements were carried out at 368 nm

Figure 6 shows the change in the absorption spectra of the ligand **(3)** with increasing concentrations of Al^{3+}. As similar to that of Hg^{2+}, there were five isosbestic points at 354, 362, 372, 382 and 392 nm indicating five equilibriums during the complexation with Al^{3+} ion. All the isosbestic points were well-pronounced in contrast with Hg^{2+}. We disclosed formation of a stable 1:1 (M:L) complex with Al^{3+} from the absorbance changes at 368 nm. Figure 6 (left inset) shows the molar ratio plot for Al^{3+}. The inflection point was 1.0 ([M]/[L]). It can thus be concluded that the ligand **(3)** formed a stable 1:1 (M:L) complex with Al^{3+}. The ratio of $A_o/(A_o - A)$ plotted versus $[M]^{-1}$ gave a good straight line. We calculated the value of log K by 4.66 for Al^{3+}-complex.

The change in the absorption spectra of the ligand **(3)** with increasing concentrations of Cu^{2+} is shown in Fig. 7. There were five isosbestic points at 354, 362, 372, 382 and 392 nm. This result indicates that there were five equilibriums in solution for Cu^{2+}. We disclosed formation of a stable 2:1 (M:L) complex with Cu^{2+} from the absorbance changes both at 368 nm and at 388 nm. As seen from Fig. 7 (inset in left), the break point is 2.0. Namely, the complex composition of Cu^{2+} was 2:1. The value of Log K was 4.90 for this complex (Fig. 7 inset in right).

Consequently, we found more isosbestic points than one during spectrophotometric titrations with the mentioned metal cations. These results show that there were many species corresponding to the absorption in the solutions. Sung et al. found similar results with an anthracene-based fluorescent PET sensor [34].

Table 1 shows complex stability constants and complex composition of ligand **(3)** with metal cations in acetonitrile–tetrahydrofuran (1/1). The values were obtained from

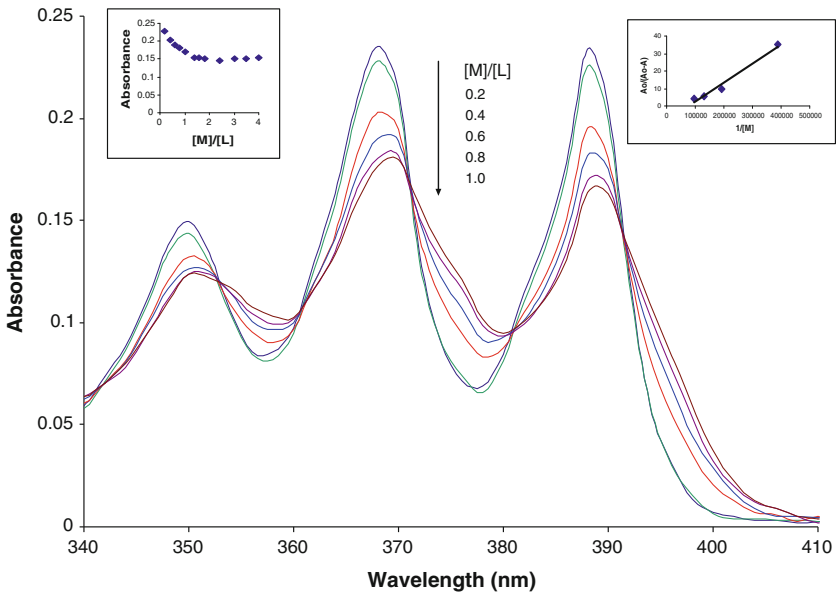

Fig. 6 Relationship of the absorbance of the ligand **(3)** with the concentration of Al^{3+}. The spectral changes during the addition of 0–1 equivalent of $Al(ClO_4)_3$. Ligand concentration: 2.58×10^{-5} M. *Insets*: Measurements were carried out at 368 nm

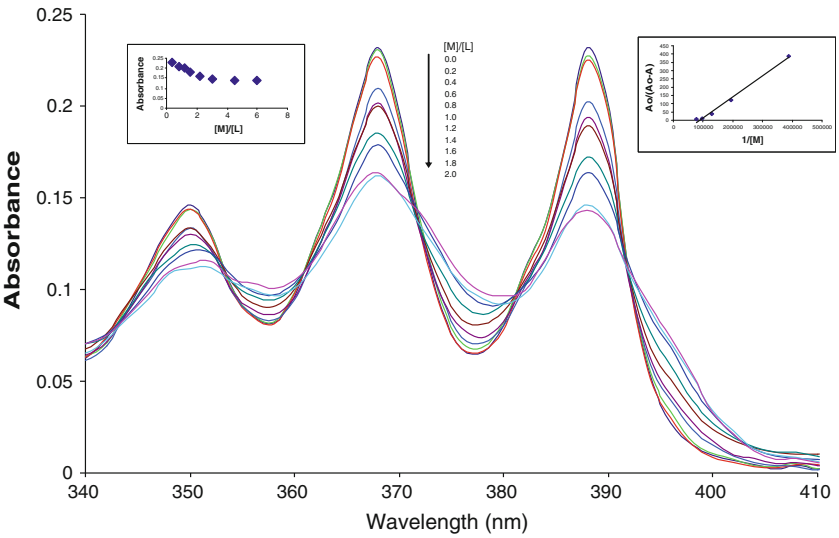

Fig. 7 Relationship of the absorbance of the ligand **(3)** with the concentration of Cu^{2+}. The spectral changes during the addition of 0–1 equivalent of $Cu(ClO_4)_2$. Ligand concentration: 2.58×10^{-5} M. *Insets*: Measurements were carried out at 368 nm

Table 1 Complex stability constants and complex composition of the ligand **(3)** with metal cations in acetonitrile–tetrahydrofuran (1/1)

Cation	Complex composition[a] (M:L)	Stability constant[a] (Log K)
Hg^{2+}	2:1	4.48 ± 0.16
Fe^{2+}	2:1	4.45 ± 0.10
Fe^{3+}	2:1	4.49 ± 0.23
Cu^{2+}	2:1	4.90 ± 0.04
Al^{3+}	1:1	4.66 ± 0.09

[a] Averages calculated from the data obtained from six independent absorbance measurements

spectrophotometric titrations. As seen from Table 1, the most stable complex is the Cu^{2+}-ligand **(3)** complex with a log K value of 4.90.

Fluorescence spectra

Excitation at 368 nm of the ligand **(3)** gives characteristic emission bands of anthracene between 380 and 450 nm. As seen from Fig. 1, fluorescence spectral behavior of the ligand **(3)** showed weak emission band at 415 nm. The emission band intensity of the ligand was reduced about 85% with respect to that of standard substance 9-chloromethyl anthracene (Fig. 1). The weak fluorescence intensity can be explained in a way that the emission of anthracene group is quenched by intramolecular photo-induced electron transfer from the lone pair of electrons of the nitrogen to the adjacent anthracene group. This result is similar to that for the classical fluorescent-azacrown system [34–36].

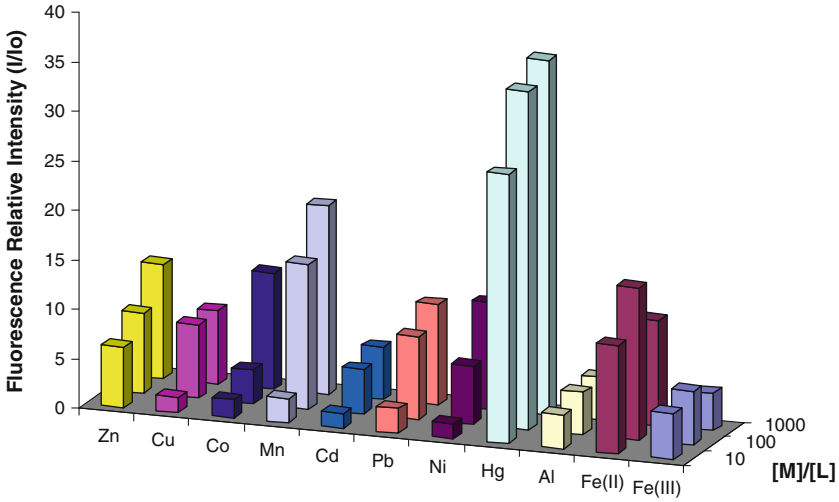

Fig. 8 Fluorescence enhancement ratios (I/Io) at 424 nm for interaction of **(3)** various metal cations in acetonitrile–tetrahydrofuran solution (1/1). Ligand concentration = 9.7×10^{-7} M. $\lambda_{ex} = 368$ nm

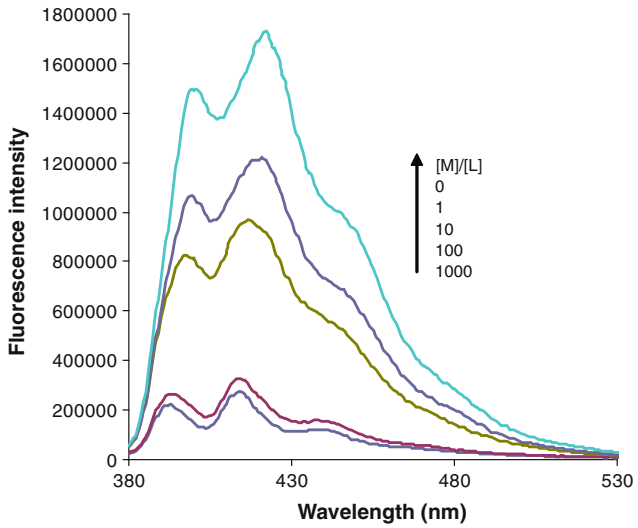

Fig. 9 Relationship of the fluorescence of the ligand **(3)** with the concentration of Zn^{2+}. The spectral changes during the addition of 0–1000 equivalents of $Zn(ClO_4)_2$. Ligand concentration = 9.7×10^{-7} M. $\lambda_{ex} = 368$ nm

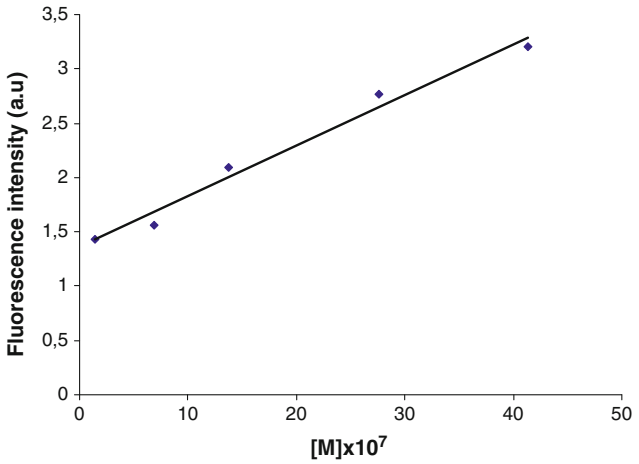

Fig. 10 Fluorescence intensity of the ligand **(3)** versus the Zn^{2+} concentration for the spectrofluorimetric titration

The fluoroionophoric properties of the ligand **(3)** were investigated by fluorescence measurements in the presence of Al^{3+}, Zn^{2+}, Fe^{2+}, Fe^{3+}, Co^{2+}, Ni^{2+}, Cu^{2+}, Cd^{2+}, Hg^{2+} and Pb^{2+} ions. Figure 8 shows the relative fluorescence intensity (I/Io) depending on the changing [M]/[L] ratio for various metal cations. When the [M]/[L] ratio changes from 10 to 1000 there was an enhancement in the fluorescence intensity of **(3)** for Zn^{2+}, Co^{2+}, Ni^{2+}, Mn^{2+}, Cd^{2+}, Hg^{2+} and Pb^{2+}. As seen from Fig. 8, there were pronounced fluorescence enhancements for Hg^{2+} with respect to other metal cations. Unfortunately, there was no sufficiently regular enhancement in the fluorescence intensity of **(3)** for the determination of this cation. However, we found regular change in the fluorescence intensity of **(3)** with Zn^{2+} (Fig. 9). The intramolecular photo-induced electron transfer to the adjacent anthracene group upon photoexcitation of the fluorophore has been hindered by Zn^{2+} binding in crown ether cavity. Therefore the complexation has caused the enhancement of the fluorescence intensity of the ligand **(3)**. A linear response of the fluorescence intensity as a function of Zn^{2+} concentration was observed from 1.4×10^{-7} to 4.1×10^{-6} M with linearly dependent coefficient $R^2 = 0.9804$ (Fig. 10). The detection limit calculated as three times the standard deviation of the blank signal was found to be 1.0×10^{-8} M.

Acknowledgment This work was supported by The Scientific and Technological Research Council of Turkey (TUBITAK).

References

1. Ropek, D., Para, A.: The effect of heavy metal ions and their complexions upon growth, sporulation and pathogenicity of the

entomopathogenic fungus paecilomyces farinosus. Polish J. Environ. Stud. **12**, 227–230 (2003)
2. Tudor, M.J., Tudor, M., David, C., Teodorof, L., Tudor, D., Ibram, O.: Chemicals as intentional and accidental global environmental threats. Springer, Netherlands (2006)
3. Pawlik-Skowronska, B.: Correlations between toxic Pb effects and production of Pb-induced thiol peptides in the microalga Stichococcus bacillaris. Environ. Pollut. **119**, 119–127 (2002)
4. Vosyliene, M.Z., Jankaite, A.: Effect of heavy metal model mixture on rainbow trout biological parameters. Ekologija **4**, 12–17 (2006)
5. Shah, S.L., Altındağ, A.: Effects of heavy metal accumulation on the 96-h LC50 values in Tench Tinca tinca L.1758. Turk. J. Vet. Anim. Sci. **29**, 139–144 (2005)
6. Ansari, T.M., Marr, I.L., Tariq, N.: Heavy metals in marine pollution perspective-A mini review. J. Appl. Sci. **4**(1), 1–20 (2004)
7. Goodman, W.G.: Pathophysiologic mechanisms of aluminum toxicity aluminum-induced bone disease. In: de Broe, M.E., Coburn, J.W. (eds.) Aluminum and Renal Failure. Kluwer Academic Publishers, Dordrecht, Boston, London (1990)
8. Rogers, M.A., Simon, D.G.: A preliminary study of dietary aluminum intake and risk of Alzheimer disease. Age Ageing **28**, 205–209 (1999)
9. Nagasawa, K., Akagi, J., Koma, M., Kakuda, T., Nagai, K., Shimohama, S., Fujimoto, S.: Transport and toxic mechanism for aluminum citrate in human neuroblastoma SH-SY5Y cells. Life Sci. **79**, 89–97 (2006)
10. Thompson, R.B., Peterson, D., Mahoney, W., Cramer, M., Maliwal, B.P., Suh, S.W., Frederickson, C., Fierke, C., Herman, P.: Fluorescent zinc indicators for neurobiology. J. Neurosci. Methods **118**, 63–75 (2002)
11. Shay, N.F., Mangian, H.F.: Neurobiology of zinc-influenced eating behavior. J. Nutr. **130**, 1493S–1499S (2000)
12. Yang, D.Y., Lee, J.B., Lin, M.C., Huang, Y.L., Liu, H.W., Liang, Y.J., Cheng, F.C.: The determination of brain magnesium and zinc levels by a dual-probe microdialysis and graphite furnace atomic absorption spectrometry. J. Am. Coll. Nutr. **23**(5), 552S–555S (2004)
13. Garcia, E.A., Gomis, D.B.: Sequential extraction spectrofluorimetric determination of ultratraces of zinc using cryptand 2.2.1 and eosin. Mikrochim. Acta **124**, 179–185 (1996)
14. Shemirani, F., Rajabi, M., Asghari, A., Milani-Hosseini, M.R.: Simultaneous determination of traces of cadmium and zinc by adsorptive stripping voltammetry. Can. J. Anal. Sci. Spectrosc. **50**(4), 176–181 (2005)
15. Reza, G., Khaniki, J.: Determination of zinc contents in Iranian flat breads. Pak. J. Nutr. **4**(5), 294–297 (2005)
16. Andac, M., Asan, A., Tınkılıç, N., Işildak, I.: A simple flow-injection spectrofluorimetric method for the determination of mercury. J. Fluoresc. **17**, 401–405 (2007)
17. Xiang, Y., Mei, L., Li, N., Tong, A.: Sensitive and selective spectrofluorimetric determination of chromium(VI) in water by fluorescence enhancement. Anal. Chim. Acta **581**, 132–136 (2007)
18. Liao, W.S., Wu, F.Y., Wu, Y.M., Wang, X.J.: Highly sensitive spectrofluorimetric determination of cysteine by Cu^{2+}-morin comple. Microchim. Acta **162**, 147–152 (2008)
19. Valeur, B., Leray, I.: Desing principles of fluorescent molecular sensors for cation recognition. Coord. Chem. Rev. **205**, 3–40 (2000)
20. Izatt, R.M., Pawlak, K., Bradshaw, J.S., Bruening, R.L.: Thermodynamic and kinetic data for macrocycle interaction cations, anions and neutral molecules. Chem. Rev. **95**, 2529–2586 (1995)
21. Talanova, G.G., Roper, E.D., Buie, N.M., Gorbunova, M.G., Bartsch, R.A., Talanov, V.S.: Novel fluorogenic calix[4]arene-bis(crown-6-ether) for selective recognition of thallium(I). Chem. Commun., 5673–5675 (2005)
22. Gokel, G.W., Leevy, W.M., Weber, M.E.: Crown ethers: sensors for ions and molecular scaffolds for materials and biological models. Chem. Rev. **104**(5), 2723–2750 (2004)
23. Veggel, F.C.J.M., Verboom, W., Reinhoudt, D.N.: Metallomacrocycles: supramolecular chemistry with hard and soft metal cations in action. Chem. Rev. **94**(2), 279–299 (1994)
24. Hancock, R.D., Martell, A.E.: Ligand design for selective complexation of metal ions in aqueous solution. Chem. Rev. **89**(8), 1875–1914 (1989)
25. Xu, X., Xu, H., Ji, H.F.: New fluorescent probes for the detection of mixed sodium and potassium metal ions. Chem. Commun., 2092–2093 (2001)
26. Chang, J.H., Choi, Y.M., Shin, Y.K.: A significant fluorescence quenching of anthrylaminobenzocrown ethers by paramagnetic metal cations. Bull. Korean Chem. Soc. **22**(5), 527–530 (2001)
27. Ji, H.F., Dabestani, R., Hettich, R.L., Brown, G.M.: Optical sensing of cesium using 1, 3-alternate calix[4]-mono-and di(anthrylmethyl)aza-crown-6. Photochem. Photobiol. **70**(6), 882–886 (1999)
28. Silva, A.P., Silva, S. A.: Fluorescent signaling crown ether; Swiching on of fluorescence by alkali metal ion recognition and binding in situ. Chem. Commun., 1709–1710 (1986)
29. Ostaszewski, R., Bozek, A., Palys, M., Stojek, Z.: Complexation properties of anthracene-bridged bis-crown ethers. J. Chem. Soc., Perkin Trans. **2**, 1193–1198 (1999)
30. Ostaszewski, R., Prody, L., Montalti, M.: The synthesis and complexation studies of thia-anthracene receptors. Tetrahedron **55**, 11553–11562 (1999)
31. Bourson, J., Valeur, B.: Ion-responsive fluorescent compounds. Cation-steered intramolecular charge transfer in a crowned merocyanine. J. Phys. Chem. **93**, 3871–3876 (1989)
32. Martin, J.W.L., Organ, G.J., Wainwright, K.P., Weerasuria, K.D.V., Willis, A.C., Wild, S.B.: Copper(I) complexes of 14- and 16-membered chelating macrocycles with trans-disposed pairs of imine-N and thioether-S donors: Crystal and molecular structures of $[Cu(C_{18}H_{18}N_2S_2)]CF_3SO_3$ and $[Cu(C_{20}H_{22}N_2S_2)]CF_3SO_3$. Inorg. Chem. **26**, 2963–2968 (1997)
33. Khin, C., Lim, M.D., Tsuge, K., Iretskii, A., Wu, G., Ford, P.C.: Amine nitrosation via NO reduction of the polyamine copper(II) complex $Cu(DAC)^{2+}$. Inorg. Chem. **46**(22), 9323–9331 (2007)
34. Sung, K., Fu, H.K., Hong, S.H.: A Fe^{3+}/Hg^{2+}-selective anthracene-based fluorescent PET sensor with tridentate ionophore of amide/β-amino alcohol. J. Fluoresc. **17**, 383–389 (2007)
35. Kubo, K., Ishige, R., Sakurai, T.: Complexation and fluorescence behavior of diazacrown ether carrying two anthryl pendants. Talanta **49**, 339–344 (1999)
36. Seo, H.S., Karim, M.M., Lee, S.H.: Selective fluorimetric recognition of cesium ion by 15-crown-anthracene. J. Fluoresc. **18**, 853–857 (2008)